






## Article

# *Puccinia* Spore Concentrations in Relation to Weather Factors and Phenological Development of a Wheat Crop in Northwestern Spain

Kenia C. Sánchez Espinosa <sup>1,\*</sup> , María Fernández-González <sup>1</sup> , Michel Almaguer <sup>2</sup> , Guillermo Guada <sup>1</sup>   
and Francisco Javier Rodríguez-Rajo <sup>1</sup> 

<sup>1</sup> Department of Plant Biology and Soil Sciences, Faculty of Sciences, University of Vigo, 32004 Ourense, Spain; mfgonzalez@uvigo.es (M.F.-G.); guillermo.guada@uvigo.gal (G.G.); javirajo@uvigo.es (F.J.R.-R.)

<sup>2</sup> Department of Microbiology and Virology, Faculty of Biology, University of Habana, La Habana 10400, Cuba; michelalm@fbio.uh.cu

\* Correspondence: ksanchez8909@gmail.com

**Abstract:** Rust is one of the main diseases affecting wheat crops in Spain, causing significant yield and quality losses. Research on its identification and quantification in the air is a worldwide priority due to the importance of this crop as a source of food and feed. The objective of this study is to determine the temporal variation of airborne spores of *Puccinia* and their relationship with meteorological variables and the phenological development of a wheat crop in Northwestern Spain during two growing seasons. The study was conducted in A Limia, Ourense, located in Northwestern Spain, during the wheat growing seasons of 2021 and 2022. The Lanzoni VPPS 2010 spore trap was used to collect airborne spores, which were identified using optical microscopy. The wheat growing season was less than 95 days during both years, and wheat rust spores were detected during all phenological stages of the crop. Concentrations were higher than 100 spores/m<sup>3</sup> from the booting stage to senescence, mainly in 2021. Statistical analyses showed that temperature was the meteorological variable that most influenced *Puccinia* concentrations in the air in both years. The modification of a prediction model proposed by other authors for wheat rust, which takes into account mean temperature (10–25 °C), dew point temperature (<5 °C), and nighttime temperature (10–20 °C), allowed us to tentatively predict the increase in *Puccinia* concentrations in the year 2022 when these conditions occurred for four or five consecutive days. This research is the first in Spain to report the presence of rust-causing *Puccinia* spores in the air during all phenological stages of the wheat crop and provides useful information for designing management strategies, considering temperature values.

**Keywords:** aerobiology; airborne spores; wheat; phenology; meteorology



**Citation:** Sánchez Espinosa, K.C.; Fernández-González, M.; Almaguer, M.; Guada, G.; Rodríguez-Rajo, F.J. *Puccinia* Spore Concentrations in Relation to Weather Factors and Phenological Development of a Wheat Crop in Northwestern Spain. *Agriculture* **2023**, *13*, 1637. <https://doi.org/10.3390/agriculture13081637>

Academic Editor: Peng Zhang

Received: 26 July 2023

Revised: 15 August 2023

Accepted: 17 August 2023

Published: 19 August 2023



**Copyright:** © 2023 by the authors. Licensee MDPI, Basel, Switzerland. This article is an open access article distributed under the terms and conditions of the Creative Commons Attribution (CC BY) license (<https://creativecommons.org/licenses/by/4.0/>).

## 1. Introduction

Wheat is a staple food in all regions of the world. In most countries, common wheat (*Triticum aestivum* L.) is predominantly cultivated, with a lower production rate of durum wheat (*T. turgidum* L. ssp. durum (Desf.) Husn.) [1]. According to the records of the Food and Agriculture Organization of the United Nations (FAO), in the year 2021, Spain's wheat production amounted to 8,564,630 tons, and it imported 4,017,657.85 tons to cover national demand [2]. Bread is one of the main foods produced with this cereal in the country, and Spanish households spend 4.41% of their total expenditure on food and beverages for home on the purchase of this product. Each Spanish individual consumes an average of 30.07 kilos of bread per year [3].

Fungi are responsible for the most common wheat infections, both in the field and during post-harvest storage. Several species of *Puccinia* infect wheat crops worldwide and are considered a serious threat to its stable supply [4]. *P.* is a biotrophic pathogen belonging to the family Pucciniaceae, order Pucciniales, class Pucciniomycetes, and division

Basidiomycota. *P. striiformis* Westend. f. sp. *tritici* Erikss. (Pst) causes stripe rust, *P. triticina* Erikss. (Pt) causes leaf rust, and *P. graminis* Pers. f. sp. *tritici* Erikss. & Henning (Pgt) causes stem rust [5]. Generally, the disease occurs in the northern and southern areas of temperate regions. The leaf rust pathogen, which is the most common and widely distributed wheat rust, primarily attacks the leaf blades, although it can also infect the leaf sheath and glumes in highly susceptible cultivars [6]. Pst causes yellow streaks between leaf veins in adult plants, but urediniospores form clusters during the seedling stage of infection [7]. Pgt mainly infects stems and leaf sheaths but occasionally affects leaf blades and glumes [8]. These plant pathogens have complex (macrocytic) life cycles, involving five types of spores: urediniospores, teliospores, basidiospores, pycniospores, and aeciospores, and they are heteroecious, requiring alternative hosts to complete their life cycles [9]. Each rust species has specific environmental requirements, such as the presence of a film of water on the leaf surface from intermittent rainfall or heavy dew, as well as temperatures conducive to the germination and growth of the pathogen [10].

The phytopathogenic potential of these rust fungi may be associated with the production of a large number of spores, as well as their inter and intracontinental dissemination by wind [7]. In this regard, aerobiological studies can determine the temporal variation of spores and contribute to understanding the disease epidemiology and its control. Previous studies on the detection of *P.* conducted in the air of wheat-growing areas utilized volumetric collectors and non-viable identification methodologies [5,11–13]. By combining the aerobiological study of rust incidence and severity data with meteorological data, models for rust forecasting have been developed in Canada, the United States, Mexico, Argentina, India, Ethiopia, and Morocco [10,13–17]. Phenological studies should also be considered to define regularities in the crop's growth in relation to its environment and enable the application of disease control measures at the appropriate time [18].

In Spain, stripe rust caused high yield losses in wheat production in 1958, 1978, and 2012, while leaf rust, despite being the most common, rarely causes major problems. Stem rust has not been detected since the early 1970s, although it could be present at low frequencies, making its detection difficult [9]. In recent years, infections with leaf and stem rust in previously resistant varieties [19,20] have been observed in wheat fields in the Andalusian region. There are no records of aeromycological studies in Spanish wheat fields for the identification and quantification of *P.* spores in different growing seasons. Most of the studies are oriented to its identification in the infected plant organs [1,21]. Our study is intended to demonstrate that rust-causing *P.* spores are present in the air during the different phenological phases of wheat cultivation in Northwestern Spain and that their concentrations are affected by meteorological variations. Therefore, the objective of this study was to determine the temporal variation of airborne spores of *P.* and their relationship with meteorological variables and the phenological development of a wheat crop in Northwestern Spain during two growing seasons.

## 2. Materials and Methods

The sampling site was a wheat (*Triticum aestivum*) plantation of the Galician autochthonous variety Caaveiro, located in A Limia, Ourense, Galicia, in Northwestern Spain (Figure 1). The study was conducted during two growing seasons (May–August 2021 and May–August 2022). Daily values of meteorological variables were recorded throughout the crop cycle using a portable weather station ( $\mu$ METOS CLIMA) located in the study area at a height of 1.50 m. The recorded meteorological variables included maximum, minimum, and average temperatures ( $^{\circ}$ C), dew point ( $^{\circ}$ C), relative humidity (%), rainfall (mm), wind speed (km/h), sunshine hours (h), and leaf moisture (h).



**Figure 1.** Sampling location area A Limia, Ourense, Spain.

The concentration of airborne *P.* spores was monitored using a Lanzoni VPPS 2010 trap, positioned 1.50 m above ground level. The Lanzoni spore trap sampled the air continuously throughout the observation periods. The device was calibrated to collect 10 L of air per minute, and the spores impacted onto a Melinex tape coated with a 2% silicone solution. For the collection and processing of aerobiological samples, the methodology proposed by Galán et al. [22] was employed. The spores were counted along two longitudinal sections of a microscopic slide with a 400× magnification. Each *P.* spore corresponding to the morphology of the rust-causing species (*Pst*, *Pt*, and *Pgt*) was counted as a unit. Urediniospores displaying germinating pores, equinulation, hyaline outer walls, round to obovoid shapes, and sizes ranging from 26 μm to 30 μm × 18 μm to 32 μm, with colors ranging from yellow to orange, reddish to brown, and brown to black, were quantified as *P.* (Figure S1) [5]. The results were expressed as the number of spores per cubic meter of air [23].

The BBCH scale, developed by Meier et al. [24], was used for the phenological study. This scale defines nine main growth stages (S) for cereals: S0: germination; S1: leaf development; S2: tillering; S3: stem elongation; S4: booting; S5: inflorescence emergence, heading; S6: flowering; S7: development of fruit; S8: ripening; and S9: senescence.

Spearman's rank correlation was used to determine the strength of the relationship between daily airborne spore concentrations up to three days prior and the corresponding day's meteorological variables. Significance was calculated for \*  $p < 0.05$ , using Statistica version 8.0 software (Statistica, Tulsa, OK, USA). Additionally, principal component analysis (PCA) was performed to evaluate the overall meteorological influence of all variables on *P.* concentrations. The IBM SPSS Statistics 24 package was used for the statistical analysis.

To establish a warning for the occurrence of the disease, the model developed by Rodríguez-Moreno et al. [10] was tested with modifications. The model proposes that a warning of occurrence (1) or non-occurrence (0) of the disease can be given depending on the fulfillment of specific meteorological conditions: five consecutive days with an average temperature between 10 and 25 °C, nighttime temperature (from 20:00 to 7:00) between 10 and 20 °C, and a dew point temperature greater than or equal to 5 °C. Additionally, the model by Rodríguez-Moreno et al. [10] was adapted to our study area by adjusting the nighttime temperature schedule to be from 23:00 to 7:00, as dusk during the study period occurred at approximately that time.

### 3. Results

The wheat vegetative cycle lasted 94 days in 2021 and 89 days in 2022. In 2021, S0 and S1 were identified in May with durations of seven and eight days, respectively. S2 extended from the end of May to the beginning of June, lasting 13 days. S3, S4, and S5

were detected in June, each with a duration of seven days. In July, S6 and S7 developed, lasting 13 and 14 days, respectively. S8 had the same duration as S7 and lasted from the end of July until August 10. The final stage, S9, lasted only four days in August. The most extended phenological stages in terms of time were S7 and S8. In 2022, S0 lasted seven days in May, and S1 developed from the end of May until the first day of June. S2, S3, and S4 were identified during the month of June lasting fourteen, seven, and six days, respectively. S5 lasted seven days, from the end of June to the beginning of July. S6 also lasted for the same duration in July. S7 was detected for 14 days in July, S8 lasted 7 days from the end of July to the beginning of August, and S9 lasted 13 days in the first 2 weeks of August. Stages S2 and S7 showed the longest durations (Figure 2). Crop management practices consisted of land preparation (plowing and fertilizing); planting; weed, disease, and pest control; and finally, harvesting. Herbicides and insecticides targeting slugs were applied on 13 June 2021 and 14 June 2022. Fungicides were applied on 26 June 2021 and 27 June 2022.

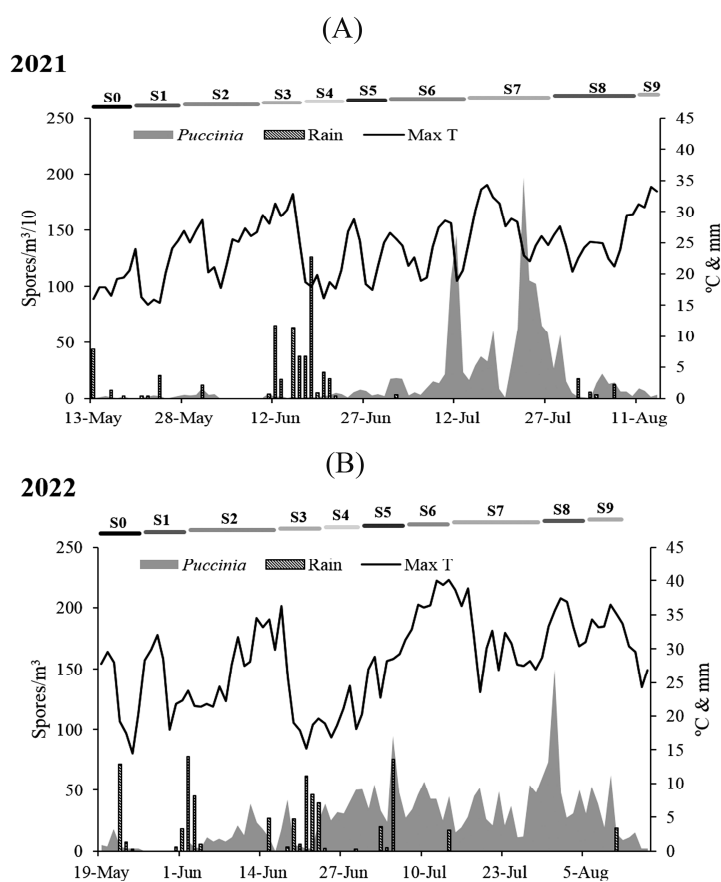


**Figure 2.** Dynamics of *Puccinia* concentrations (grey area) during 2021 (A) and 2022 (B) and daily meteorological parameters (maximum temperature shown in lines and precipitation shown in bars). In the upper part, the duration of the main phenological stages is depicted (S0: germination; S1: leaf development (main stem); S2: tillering; S3: stem elongation; S4: booting; S5: inflorescence emergence, heading; S6: flowering anthesis; S7: development of fruit; S8: ripening of fruits and seeds; S9: senescence).

*P.* concentrations were highest in 2021 at most phenological stages, particularly from S6 to S8 (Figure 2, Table 1). In both studied seasons, the highest total concentrations were detected during the month of July. In 2021, the peak value was observed at the fruit development stage (S7) on July 23 (1980 spores/m<sup>3</sup>), and in 2022, at the ripening of fruits and seeds stage (S8) on July 31 (150 spores/m<sup>3</sup>). The lowest concentrations were detected at the germination stage (S0) in 2021 (57 spores/m<sup>3</sup>) and at the germination (S0) and leaf development stage (S1) in 2022 (37 spores/m<sup>3</sup>).

**Table 1.** Total *Puccinia* concentrations at each phenological stage, maximum daily value (spores/m<sup>3</sup>), and date of maximum value during the wheat growing season in 2021 and 2022.

		S0	S1	S2	S3	S4	S5	S6	S7	S8	S9
2021	Total	57	95	243	93	151	290	3990	8114	1834	197
	Peak	20	23	92	45	46	75	1461	1980	573	90
	Peak date	15 May	23 May	31 May	11 Jun	22 Jun	26 Jun	12 Jul	23 Jul	29 Jul	11 Aug
2022	Total	37	40	37	74	148	296	592	406	461	339
	Peak	18	8	39	42	39	95	57	52	150	63
	Peak date	21 May	29 May	12 Jun	18 Jun	24 Jun	5 Jul	10 Jul	19 Jul	31 Jul	9 Aug

During the 2021 wheat growing season, the maximum temperature ranged from 18.21 to 32.30 °C, the minimum temperature from 4.18 to 11.04 °C, and the average temperature from 12.40 to 21.38 °C. Dew point values ranged from 7.71 to 14.67 °C, relative humidity ranged from 69.75 to 89.71%, and rainfall had a maximum accumulation of 38.10 mm in S4. Wind speed ranged from 6.25 to 11.07 km/h, sunshine hours ranged from 4.49 to 10.73 h, and leaf moisture ranged from 2.78 to 10.87 h. During the year 2022, the minimum and maximum values of the maximum and minimum temperatures were higher than in 2021. The maximum temperature ranged from 19.92 to 34.63 °C, the minimum temperature ranged from 6.42 to 12.34 °C, and the average temperature ranged from 13.23 to 23.64 °C. Likewise, the minimum (9.42 °C) and maximum (14.94 °C) dew point values were higher in 2022 compared to 2021. The extreme values of relative humidity (63.29–84.43%), cumulative rainfall (0–27.90 mm), and leaf moisture (2.04 and 8.17 h) were lower in 2022. Wind speed ranged between 7.44 and 8.99 km/h, and sunshine hours fluctuated between 5.36 and 10.53 h (Table 2).

**Table 2.** Main meteorological parameters—daily mean values of maximum, minimum, and average temperatures (Max T, Min T, Avg T °C), dew point (°C), relative humidity (RH%), accumulated rain (mm), wind speed (m/s), sun hours (h), and leaf moisture (h) during the phenological stages (S0: germination; S1: leaf development; S2: tillering; S3: stem elongation; S4: booting; S5: inflorescence emergence, heading; S6: flowering; S7: development of fruit; S8: ripening; S9: senescence).

		S0	S1	S2	S3	S4	S5	S6	S7	S8	S9
2021	Max T	18.21	19.53	24.52	29.47	18.53	23.30	23.58	27.96	24.79	32.30
	Min T	5.99	4.18	6.78	11.04	9.86	7.83	9.13	10.41	8.75	9.43
	Avg T	12.40	12.44	16.06	19.39	13.47	15.89	16.42	19.29	16.75	21.38
	Dew Point	9.33	7.71	11.16	14.67	11.64	11.27	12.21	13.41	12.15	14.00
	RH	84.14	76.38	76.54	78.71	89.71	77.57	79.23	74.57	77.93	69.75
	Rain	9.60	4.40	2.10	33.60	38.10	0.00	0.60	0.00	6.90	0.00
	Wind Speed	10.73	8.31	8.09	7.84	11.07	7.64	8.89	7.52	8.16	6.25
	Sun Hours	5.51	8.01	9.26	8.37	4.49	8.73	7.12	8.29	7.71	10.73
	Leaf Moisture	3.34	2.78	7.07	10.87	9.54	5.01	6.64	7.99	8.11	10.00
2022	Max T	22.41	25.83	26.67	23.24	19.92	24.80	34.63	32.64	32.44	31.67
	Min T	7.90	8.31	10.94	11.20	6.42	9.21	11.33	11.83	11.16	12.34
	Avg T	15.44	17.46	18.38	16.71	13.23	16.76	23.64	22.29	22.33	21.52
	Dew Point	11.43	11.50	14.44	13.39	9.42	12.41	13.83	14.35	13.89	14.94
	RH	80.43	73.57	82.07	84.43	81.00	79.57	63.29	68.29	66.00	72.23
	Rain	14.50	3.90	27.90	25.70	7.50	18.00	0.00	3.10	0.00	3.40
	Wind Speed	8.99	7.44	7.71	8.83	8.92	8.50	7.56	8.99	8.84	8.61
	Sun Hours	5.69	7.37	6.95	5.36	6.45	6.76	10.53	9.49	10.07	8.88
	Leaf Moisture	5.53	6.87	8.17	6.33	5.28	6.17	4.97	2.04	2.63	2.05

The influence of the main meteorological variables up to three days before on the presence of *P.* in the air at each stage was also statistically evaluated by means of a Spearman correlation test (Table S1). During the year 2021, *P.* spores showed a significant and positive correlation with the average temperature and dew point on the same day and in the three



preceding days, with the maximum temperature on the same day and the two preceding days, and with the minimum temperature on the same day and three days before. A negative correlation with the same level of significance was detected between *P.* spores and the rainfall of the same day and during the three preceding days. In the year 2022, the analysis showed a significant and positive degree of association between *P.* spores and the maximum and average temperature, sunshine hours on the same day and one and two days before, the minimum temperature and dew point on the same day and one day before, and with the wind speed on the same day. In contrast, negative correlations were registered with the relative humidity and rainfall on the same day and one and two days before, as well as with the leaf moisture on the same day and one day before.

When the correlations by stage were assessed during the year 2021, we observed that during the S0 stage, *P.* concentrations were positively correlated with wind speed three days earlier. In S2, there was a positive correlation with leaf moisture one and two days earlier. In S4, the spore concentrations were negatively correlated with the minimum temperature two days earlier, dew point two and three days earlier, and rainfall one day earlier. In S5, there was a positive correlation with the maximum temperature two days before as well as and with the dew point and leaf moisture one day before. However, at this same stage, there was a negative correlation with the minimum temperature three days before, relative humidity two days before, and wind speed two days before. In S6, all significant correlations of spores with meteorological variables (minimum and average temperature of the previous day, dew point and hours of sunshine of the day before, and leaf moisture of three days before) were negative. In S7, there was only a negative correlation with relative humidity. During S8, a positive correlation with the maximum and average temperatures two days before, and the dew point two and three days before, was detected (Table S1).

The correlations by stage during the year 2022 showed a significant positive degree of association during S0 between *P.* spore concentrations and the maximum temperature of the previous day, average temperature, and sunshine hours two days earlier. Negative values were observed for relative humidity and rainfall one day earlier. In S1, spore values were positively correlated with the maximum temperature of two days before, average temperature on the same day, and leaf moisture of two days before, whereas they were negatively correlated with the dew point and relative humidity of the previous day. The highest number of significant correlations was detected in S2, where *P.* spore concentrations showed a positive degree of association with the maximum and average temperatures and dew point on the same day and one to three days before, minimum temperature up to two days before, and hours of sunshine on the same day and three days before. Negative correlations were found with relative humidity on the same day, rainfall on the same day and up to three days before, and leaf moisture on the same day and up to two days before. In S3, a positive correlation was observed with the minimum temperature, dew point, and wind speed one day before. The airborne spore concentrations were negatively correlated with rainfall one day before. In S4, a negative correlation was detected with the minimum temperature two days before, while a positive correlation was found with hours of sunshine two days before. In S8, there was only a negative correlation with the minimum temperature three days before, and a positive correlation with wind speed two days before. The same correlation for wind speed two days before was detected in S9, as well as the average temperature (Table S1).

A principal component analysis was performed to better understand the combined influence of all meteorological variables with *P.* airborne spores (Figure 3). Three principal components (PCs) were extracted in 2021 and 2022, as they had eigenvalues greater than or equal to 1.0, accounting for approximately 79% of the variability in the original data. Generally, the three 2021 PCs were correlated as follows: component 1 (maximum and average temperature, relative humidity, wind speed, and sunshine hours), component 2 (*P.* spores, minimum temperature, and dew point), and component 3 (rainfall and leaf moisture). Overall, in 2022, the three PCs correlated as follows: component 1 (*P.* spores, maximum and average temperature, relative humidity, rainfall, and sun hours), component 2 (minimum

temperature and dew point), and component 3 (wind speed and leaf moisture). The PCA reaffirmed that minimum, maximum, or average temperatures were the variables that positively modulated spore concentrations in both years. Similar to the total correlations, in 2021, the presence of spores was positively influenced by the maximum and average temperatures and dew point. In 2022, spore concentrations were positively correlated with maximum and average temperatures and sunshine hours, but negatively influenced by rainfall and relative humidity. The combination of increased sunshine hours and reduced relative humidity in 2022 led to a decrease in *P.* concentrations.

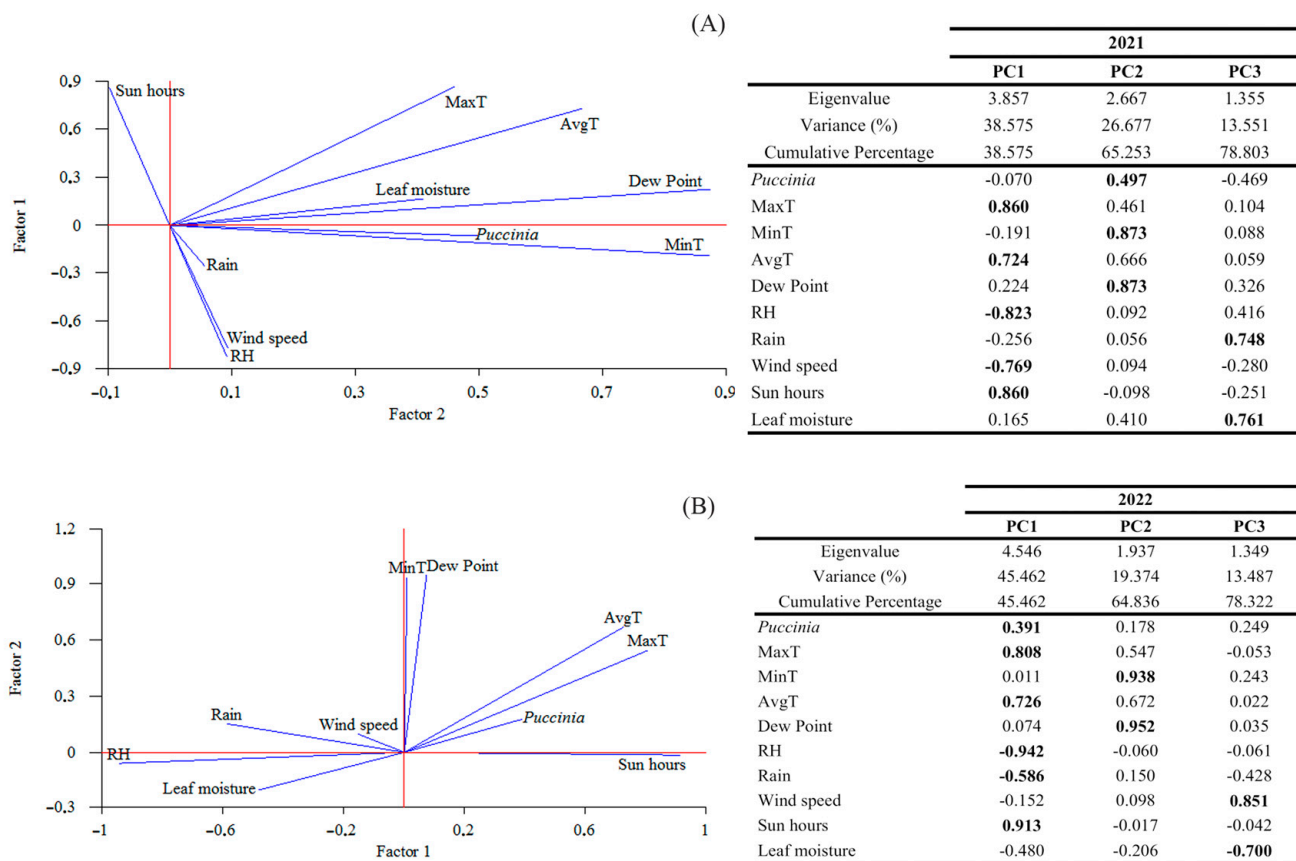


**Figure 3.** Principal component analysis for each year, 2021 (A) and 2022 (B). Principal component one (PC1), principal component two (PC2), and principal component three (PC3). Significance level in bold type ( $p < 0.05$ ).

Finally, the model developed by Rodriguez-Moreno et al. [10] for predicting leaf rust and yellow rust in wheat was applied, considering the values of average temperature, dew point, and nighttime temperature in two different time intervals: 20:00–7:00 and 23:00–7:00 (Table S2). The results indicate that this model could have provided a warning of *P.* disease occurrence in wheat from July 2 to 7, in 2022. This timeframe aligns with phenological stages S5 and S6, during which *P.* concentrations in the air began to rise above 200 spores/m<sup>3</sup>. However, this model did not account for the increase in *P.* concentrations observed in 2021.

#### 4. Discussion

Rust commonly affects wheat-growing regions in various geographical locations [5,12,14,25]. Under favorable conditions for disease development, rust can cause significant yield and quality losses [26]. The virulence profiles of the main rust-causing species, namely *P. striiformis* f. sp. *tritici*, *P. triticina*, and *P. graminis* f. sp. *tritici*, are studied to minimize the threat posed by these continuously evolving pathogens [8,27,28]. Although aeromycological studies for the identification and quantification of *P.* are limited

and nonexistent in Spain, they could contribute to the early prevention of diseases caused by these airborne pathogens, reducing their frequency and severity. Rust spores are aerodynamically ultralight and produced in unquantified quantities; they can be spread by wind and convection currents, assuring long-distance dissemination. Additionally, these spores are pigmented and possess thick walls that protect them from UV radiation, allowing them to remain viable during transport over long distances [29]. Quantifying airborne inoculum or estimating it through a predictive model based on meteorological conditions can be useful in avoiding the overestimation of disease risk and ensuring the timely application of fungicides at the correct time [12].

In our study, a non-viable volumetric sampler was utilized to collect fungal propagules, similar to other research conducted on wheat crops in different regions [12,14,30]. Research focused on identifying and quantifying airborne wheat pathogens is a global priority due to the significance of this crop as a source of food and feed [5]. The collection orifice of the Lanzoni VPPS 2010 sampler was positioned 1.75 m above the soil surface, which is suitable for sampling pathogens that may affect the flag and penultimate leaves and the bud. The fungal identification of the obtained samples using this sampler was performed through direct microscopy, employing morphological criteria that do not allow for distinguishing between the three rust-causing species in wheat. Araujo et al. [5] employed this identification methodology, which requires relatively low technological capabilities, and stated that although it is less sensitive compared to molecular techniques, it is suitable for detecting airborne *P.*

*P.* concentrations in the cultivation area were detected during all phenological phases in both 2021 and 2022, with concentrations exceeding 100 spores/m<sup>3</sup> from the boot to the senescence phase (June to August). These concentrations surpass the threshold level of urediniospores required for the development of yellow rust, the most common rust in Spain, under controlled environments and under field conditions [31]. In Lethbridge, Canada, *P.* spores were also detected throughout the growing season in 2015 and 2016, with peaks mainly in June, July, and August [13]. In the Walloon region, Belgium, *Pt* was identified in the air from S3 onwards, after the flag leaf of wheat had fully emerged in April, May, or June, during the years 2009–2012 [12]. In Gangu, Northwestern China, the highest *Pst* concentrations were detected from lateral shoot formation to fruit development [32]. Similarly, in the same country, Hu et al. [33] recently reported the presence of *Pst* from March to December, with peak concentrations in May and June, over the course of three years of monitoring. Therefore, in order to determine the appropriate timing for fungicide application, it is necessary to establish the temporal variation of the pathogen in the cultivation area over multiple years, which, based on the obtained results in our study area, tentatively ranges from S4 to S8.

On the other hand, weather conditions could have influenced the presence of *P.* throughout the growing season. Temperature plays a vital role in the interaction system between host plants and pathogens and represents one of the risks to the long-term sustainability of agriculture [25]. *Pst*, *Pt*, and *Pgt* require temperatures between 10 and 25 °C to complete their life cycle and infect wheat plants [9]. In our study, higher temperatures were recorded during the month of July in 2022, which could impact fungal development. Thus, increasing global temperatures could constrain the development and survival of *P.* in certain wheat-producing regions. In this context, Camacho et al. [29] state that there is evidence that the rise in mean annual temperature has led to a reduction in both the frequency and severity of epidemics caused by this phytopathogen.

The optimal temperature for infection and development of stripe rust is 10 °C, while for leaf rust, it is 20 °C, and for stem rust, it is 25 °C [9]. In the case of *Pt*, which causes leaf rust, leaf moisture is also necessary for infection to occur [34]. We observed higher average temperature values in 2021. In this regard, the correlation analysis of *P.* concentrations with meteorological variables revealed that the temperature of the same day and preceding days, as well as the dew point, were the variables that positively influenced spore concentrations in both years. In 2021, these variables were also found to have an impact on the presence



of this phytopathogen when considering the analysis of all meteorological variables on its concentrations, whereas in 2022, only temperature showed a significant correlation. Duvivier et al. [12] demonstrated through multiple regression analysis that low winter temperatures positively influence the spore density of *P. triticina* between the onset of stem elongation and the flag leaf stage at the S3 stage. Similarly, Newlands [13] suggests that Pst becomes dormant for longer periods as nighttime temperatures become colder, because colder temperatures favor the germination of urediniospores. However, at the booting stage in both years of sampling, *P.* concentrations were negatively correlated with the minimum temperature two days earlier.

Alternatively, rainfall was negatively correlated with the presence of *P.* in both years, 2021 and 2022, which could be attributed to the washout effect of the atmosphere. The relationship between rain and rust spore dispersal is quite complex [35]. Field and in vitro experiments have shown that rainy periods promote the release of spores from infected plants, but also decrease the concentrations of spores in the air that can be deposited on susceptible plants [36]. Moreover, if rainfall events are extensive or heavy, they can reduce the number of spores deposited on the leaves, thereby limiting the progression of the disease [37].

The correlation between *P.* concentrations and wind speed was positive in most of the phenological stages where it was detected, as well as in 2022 with total concentrations. Similar results have been obtained by other researchers, who point out that this correlation varies depending on wind direction [29]. The influence of this meteorological variable may favor the dispersion of fungal propagules over long distances, and spores from other regions may be detected. Hovmøller et al. [38] reported that *P. striiformis* f.sp. *tritici*, the cause of wheat stripe rust, migrates frequently between the United Kingdom, Germany, France, and Denmark. Additionally, they demonstrated through a phylogeographic analysis the existence of a single clonal population of this species in the four countries, separated by a distance of up to 1700 km.

The analysis of the combined effect of all meteorological variables on *P.* concentrations enabled us to ascertain that in the year 2022, hours of sunshine and relative humidity also played a significant role in its detection. An increase in sunshine hours leads to higher temperatures, which are suboptimal for *P.* development. On the other hand, relative humidity is known to be the primary factor influencing the development of leaf rust in wheat [39]. High humidity is optimal for stripe rust infection [40], while lower humidity promotes the spread of stem rust, which could have been predominant in 2021 and explains the negative association with humidity [41].

Based on these factors, it can be inferred that temperature was the primary factor influencing the dynamics of *P.* during both study periods, as has been demonstrated in other research studies in the northern hemisphere [11–13].

The severity of rust epidemics depends on the timing of infection by the primary inoculum, plant resistance, and the climatic conditions [13]. Various disease models with different levels of complexity and data requirements have been developed worldwide to predict rust progression in wheat [10,13–17]. These models are site-specific, due to the climatic variability that affects spore dispersal and deposition. Data from multiple years are necessary to develop a predictive model, and this study serves as an initial contribution to future rust forecasts in the studied region. We attempted to fit the model of Rodriguez-Moreno et al. [10]. For this purpose, we modified the range of nighttime temperature hours from 20:00–7:00 to 23:00–7:00, based on the climatic conditions of the study area during this period when it gets dark later. The fit showed that average temperatures between 10 and 25 °C, dew point temperatures above 5 °C, and nighttime temperatures between 10 and 20 °C for five consecutive days could predict an increase in *P.* concentrations in 2022, indicating an increased probability of wheat rust occurrence and the optimal time for fungicide application. In 2021, this model could not predict disease occurrence when considering average temperature, dew point, and nighttime conditions for five consecutive days. However, if the alert is given when these conditions exist for four consecutive days,

the disease is predicted, as it coincides with phenological stages S6 and S7, where the highest concentrations of *P.* were detected in the air. Therefore, we propose that for our study area, this model could be applied by considering the average temperature, dew point, and nighttime values proposed by Rodríguez-Moreno et al. [10] for four or five consecutive days. This approach could improve the timeliness and efficiency of fungicide applications, minimizing economic costs, environmental impact, and yield losses in the growing area.

## 5. Conclusions

Spore concentrations were highest in 2021 and were primarily influenced by the recorded temperature values. Further monitoring of this cultivation area is necessary to enhance our understanding of *P.* aerobiology and to establish more effective practices for fungicide use, which can reduce production costs and protect the environment. Tentatively, a rust alert system could be applied in this cultivation area, considering the modifications we have made to the model proposed by Rodríguez-Moreno et al. [10].

**Supplementary Materials:** The following supporting information can be downloaded at: <https://www.mdpi.com/article/10.3390/agriculture13081637/s1>, Figure S1: Photomicrographs of *Puccinia* uredinospores quantified in some of the aerobiological samples collected with the Lanzoni VPPS 2010 sampler during the study period in the wheat crop of A Limia, Ourense, Spain. 400× magnification. Table S1. Spearman's correlation between *Puccinia* concentration and weather parameters, maximum, minimum and average temperatures (Max T, Min T, Avg T °C), dew point (°C), relative humidity (RH%), accumulated rain (mm), wind speed (m/s), sun hours (h), and leaf moisture (h); during the same day and the 1, 2, and 3 previous days in each phenological stage (S0: germination; S1: leaf development (main stem); S2: tillering; S3: stem elongation; S4: booting; S5: inflorescence emergence, heading; S6: flowering anthesis; S7: development of fruit; S8: ripening of fruits and seeds; S9: senescence). Significance level in bold type ( $p < 0.05$ ). Table S2. Consecutive days in which the meteorological conditions of the Rodríguez-Moreno et al. [10] model is met during our study period. \* Nocturnal temperature of the Rodríguez-Moreno et al. [10] model.

**Author Contributions:** Conceptualization, M.F.-G. and F.J.R.-R.; methodology, M.F.-G. and K.C.S.E.; formal analysis, K.C.S.E., M.F.-G., M.A., G.G. and F.J.R.-R.; data curation, K.C.S.E.; writing—original draft preparation, K.C.S.E.; writing—review and editing, K.C.S.E., M.F.-G., M.A., G.G. and F.J.R.-R.; supervision, M.A. and F.J.R.-R. All authors have read and agreed to the published version of the manuscript.

**Funding:** This work was supported by the European Commission Horizon 2020 project SoildiverAgro [grant agreement 817819].

**Institutional Review Board Statement:** Not applicable.

**Data Availability Statement:** The datasets generated and/or analyzed during the current study are available from the corresponding author on reasonable request.

**Conflicts of Interest:** The authors declare no conflict of interest.

## References

1. Martínez-Moreno, F.; Giraldo, P.; Nieto, C.; Ruiz, M. Resistance to leaf and yellow rust in a collection of Spanish bread wheat landraces and association with ecogeographical variables. *Agronomy* **2022**, *12*, 187. [CrossRef]
2. Food and Agriculture Organization of the United Nations. Available online: <https://www.fao.org/faostat/en/#data/QCL> (accessed on 4 August 2023).
3. Ministerio de Agricultura, Pesca y Alimentación. Informe de Consumo Alimentario en España 2021. 2021. Available online: [https://www.mapa.gob.es/es/alimentacion/temas/consumo-tendencias/informe-consumo-alimentario-2021-baja-res\\_tcm30-624017.pdf](https://www.mapa.gob.es/es/alimentacion/temas/consumo-tendencias/informe-consumo-alimentario-2021-baja-res_tcm30-624017.pdf) (accessed on 4 August 2023).
4. Rodríguez-Algaba, J.; Hovmöller, M.S.; Villegas, D.; Cantero-Martínez, C.; Jin, Y.; Justesen, A.F. Two indigenous *Berberis* species from Spain were confirmed as alternate hosts of the yellow rust fungus *Puccinia striiformis* f. sp. *tritici*. *Plant Dis.* **2021**, *105*, 2281–2285. [CrossRef] [PubMed]
5. Araujo, G.T.; Amundsen, E.; Frick, M.; Gaudet, D.A.; Aboukhaddour, R.; Selinger, B.; Thomas, J.; Laroche, A. Detection and quantification of airborne spores from six important wheat fungal pathogens in southern Alberta. *Can. J. Plant Pathol.* **2021**, *43*, 439–454. [CrossRef]

6. Huerta-Espino, J.; Singh, R.P.; German, S.; McCallum, B.D.; Park, R.F.; Chen, W.Q.; Bhardwaj, S.C.; Goyeau, H. Global status of wheat leaf rust caused by *Puccinia triticina*. *Euphytica* **2011**, *179*, 143–160. [[CrossRef](#)]
7. Mehmood, S.; Sajid, M.; Zhao, J.; Huang, L.; Kang, Z. Alternate Hosts of *Puccinia striiformis* f. sp. *tritici* and Their Role. *Pathogens* **2020**, *9*, 434. [[PubMed](#)]
8. Leonard, K.J.; Szabo, L.J. Stem rust of small grains and grasses caused by *Puccinia graminis*. *Mol. Plant Pathol.* **2005**, *6*, 99–111. [[CrossRef](#)]
9. Martínez-Moreno, F.; Solís, I. Wheat rust evolution in Spain: An historical review. *Phytopathol. Mediterr.* **2019**, *58*, 3–16.
10. Rodríguez-Moreno, V.M.; Jiménez-Lagunes, A.; Estrada-Avalos, J.; Mauricio-Ruvalcaba, J.E.; Padilla-Ramírez, J.S. Weather-data-based model: An approach for forecasting leaf and stripe rust on winter wheat. *Meteorol. Appl.* **2020**, *27*, e1896. [[CrossRef](#)]
11. Eversmeyer, M.G.; Kramer, C.L. Vertical concentrations of fungal spores above wheat fields. *Grana* **1987**, *26*, 97–102. [[CrossRef](#)]
12. Duvivier, M.; Dedeurwaerder, G.; Bataille, C.; De Proft, M.; Legrève, A. Real-time PCR quantification and spatio-temporal distribution of airborne inoculum of *Puccinia triticina* in Belgium. *Eur. J. Plant Pathol.* **2016**, *145*, 405–420. [[CrossRef](#)]
13. Newlands, N.K. Model-based forecasting of agricultural crop disease risk at the regional scale, integrating airborne inoculum, environmental, and satellite-based monitoring data. *Front. Environ. Sci.* **2018**, *6*, 63. [[CrossRef](#)]
14. Moschini, R.C.; Pérez, B.A. Predicting wheat leaf rust severity using planting date, genetic resistance, and weather variables. *Plant Dis.* **1999**, *83*, 381–384. [[CrossRef](#)]
15. El Jarroudi, M.; Lahlali, R.; Kouadio, L.; Denis, A.; Belleflamme, A.; El Jarroudi, M.; Boulif, M.; Mahyou, H.; Tychon, B. Weather-based predictive modeling of wheat stripe rust infection in Morocco. *Agronomy* **2020**, *10*, 280. [[CrossRef](#)]
16. Sandhu, S.K.; Tak, P.S.; Pannu, P.P.S. Forewarning of stripe rust (*Puccinia striiformis*) of wheat in central zone of Punjab. *J. Agrometeorol.* **2021**, *23*, 435–441. [[CrossRef](#)]
17. Salotti, I.; Bove, F.; Rossi, V. Development and validation of a mechanistic, weather-based model for predicting *Puccinia graminis* f. sp. *tritici* infections and stem rust progress in wheat. *Front. Plant Sci.* **2022**, 1761.
18. Cortiñas Rodríguez, J.A.; González-Fernández, E.; Fernández-González, M.; Vázquez-Ruiz, R.A.; Aira, M.J. Fungal diseases in two north-west Spain vineyards: Relationship with meteorological conditions and predictive aerobiological model. *Agronomy* **2020**, *10*, 219. [[CrossRef](#)]
19. Vazquez, J.N.R.; Ammar, K.; Solís, I.; Martínez-Moreno, F. Virulence of *Puccinia triticina* and *Puccinia tritici-duri* on durum wheat in southern Spain, from 2020 to 2022. *Phytopathol. Mediterr.* **2023**, *62*, 29–34.
20. Olivera, P.D.; Villegas, D.; Cantero-Martínez, C.; Szabo, L.J.; Rouse, M.N.; Luster, D.G.; Jin, Y. A unique race of the wheat stem rust pathogen with virulence on Sr31 identified in Spain and reaction of wheat and durum cultivars to this race. *Plant Pathol.* **2022**, *71*, 873–889. [[CrossRef](#)]
21. Martínez, F.; Sillero, J.C.; Rubiales, D. Pathogenic specialization of *Puccinia triticina* in Andalusia from 1998 to 2000. *J. Phytopathol.* **2005**, *153*, 344–349. [[CrossRef](#)]
22. Galán, C.; Cariñanos, P.; Alcázar, P.; Dominguez, E. Management and Quality Manual. In *Spanish Aerobiology Network (REA)*; Servicio Publicaciones Universidad de Córdoba: Córdoba, Spain, 2007.
23. Galán, C.; Ariatti, A.; Bonini, M.; Clot, B.; Crouzy, B.; Dahl, A.; Fernandez-González, D.; Frenguelli, G.; Gehrig, R.; Isard, S.; et al. Recommended terminology for aerobiological studies. *Aerobiologia* **2017**, *33*, 293–295. [[CrossRef](#)]
24. Meier, U. *BBCH-Monograph: Growth Stages of Mono- and Dicotyledonous Plants*, 2nd ed.; Technical Report; Federal Biological Research Centre for Agriculture and Forestry: Rome, Italy, 2001; p. 158.
25. Hu, Y.; Su, C.; Zhang, Y.; Li, Y.; Chen, X.; Shang, H.; Hu, X. A *Puccinia striiformis* f. sp. *tritici* effector inhibits high-temperature seedling-plant resistance in wheat. *Plant J.* **2022**, *112*, 249–267. [[PubMed](#)]
26. Terefe, T.G.; Visser, B.; Pretorius, Z.A.; Boshoff, W.H.P. Physiologic races of *Puccinia triticina* detected on wheat in South Africa from 2017 to 2020. *Eur. J. Plant Pathol.* **2022**, *165*, 1–15. [[CrossRef](#)]
27. Villegas, D.; Bartaula, R.; Cantero-Martínez, C.; Luster, D.; Szabo, L.; Olivera, P.; Berlin, A.; Rodríguez-Algaba, J.; Hovmöller, M.S.; McIntosh, R.; et al. Barberry plays an active role as an alternate host of *Puccinia graminis* in Spain. *Plant Pathol.* **2022**, *71*, 1174–1184. [[CrossRef](#)]
28. Porras, R.; Miguel-Rojas, C.; Pérez-de-Luque, A.; Sillero, J.C. Macro- and Microscopic Characterization of Components of Resistance against *Puccinia striiformis* f. sp. *tritici* in a Collection of Spanish Bread Wheat Cultivars. *Agronomy* **2022**, *12*, 1239.
29. Camacho, I.; Leça, R.; Sardinha, D.; Camacho, R.; Sadyś, M. Occurrence of *Puccinia* spp. spores in Madeira Island and their phytopathological importance. *Eur. J. Plant Pathol.* **2018**, *150*, 955–969. [[CrossRef](#)]
30. Hassine, M.; Siah, A.; Hellin, P.; Cadalen, T.; Halama, P.; Hilbert, J.L.; Hamada, W.; Baraket, M.; Yahyaoui, A.; Legreve, A.; et al. Sexual reproduction of *Zymoseptoria tritici* on durum wheat in Tunisia revealed by presence of airborne inoculum, fruiting bodies and high levels of genetic diversity. *Fungal Biol.* **2019**, *123*, 763–772. [[CrossRef](#)] [[PubMed](#)]
31. De Araujo, G.T. *Determination of the Incidence of Fungal Spores for Important Wheat Pathogens in Western Canada*; University of Lethbridge: Lethbridge, AB, Canada, 2018.
32. Gu, Y.; Li, Y.; Wang, C.; Chu, B.; Liu, Q.; Luo, Y.; Ma, Z. Inter-seasonal and altitudinal inoculum dynamics for wheat stripe rust and powdery mildew epidemics in Gangu, Northwestern China. *Crop Prot.* **2018**, *110*, 65–72. [[CrossRef](#)]
33. Hu, X.; Fu, S.; Li, Y.; Xu, X.; Hu, X. Dynamic of *Puccinia striiformis* f. sp. *tritici* Urediniospore in Longnan, a Critical Overwintering Region of China. *Plant Dis.* **2023**, *10*, 1094. [[CrossRef](#)]
34. Bolton, M.D.; Kolmer, J.A.; Garvin, D.F. Wheat leaf rust caused by *Puccinia triticina*. *Mol. Plant Pathol.* **2008**, *9*, 563–575. [[CrossRef](#)]

35. Nagarajan, S.U.; Singh, D.V. Long-distance dispersion of rust pathogens. *Annu. Rev. Phytopathol.* **1990**, *28*, 139–153. [[CrossRef](#)]
36. Geagea, L.; Huber, L.; Sache, I.; Flura, D.; McCartney, H.A.; Fitt, B.D. Influence of simulated rain on dispersal of rust spores from infected wheat seedlings. *Agric. For. Meteorol.* **2000**, *101*, 53–66. [[CrossRef](#)]
37. Sache, I. Short-distance dispersal of wheat rust spores. *Agronomie* **2000**, *20*, 757–767. [[CrossRef](#)]
38. Hovmøller, M.S.; Justesen, A.F.; Brown, J.K.M. Clonality and long-distance migration of *Puccinia striiformis* f. sp. *tritici* in north-west Europe. *Plant Pathol.* **2002**, *51*, 24–32.
39. Torres-Cruz, M.M.; Fuentes-Dávila, G.; Félix-Valencia, P. Influence of the temperature and relative humidity on the incidence of wheat leaf rust (*Puccinia triticina* Eriks.) in southern Sonora, Mexico, during three crop seasons. *World J. Adv. Res. Rev.* **2022**, *14*, 200–207. [[CrossRef](#)]
40. Sørensen, C.K.; Thach, T.; Hovmøller, M.S. Evaluation of spray and point inoculation methods for the phenotyping of *Puccinia striiformis* on wheat. *Plant Dis.* **2016**, *100*, 1064–1070. [[CrossRef](#)] [[PubMed](#)]
41. Volkova, G.V.; Gladkova, E.V.; Miroshnichenko, O.O. Effectiveness of growing wheat-variety blends in reducing damage caused by stem-rust (*Puccinia graminis* pers. f. sp. *tritici* Erikss. et Henn., the Causal Agent). *Russ. Agric. Sci.* **2021**, *47*, 490–494. [[CrossRef](#)]

**Disclaimer/Publisher’s Note:** The statements, opinions and data contained in all publications are solely those of the individual author(s) and contributor(s) and not of MDPI and/or the editor(s). MDPI and/or the editor(s) disclaim responsibility for any injury to people or property resulting from any ideas, methods, instructions or products referred to in the content.